



Pal, A., Tan, C. M., & Beach, M. A. (2004). Comparison of MIMO channels from multipath parameter extraction and direct channel measurements. In International Symposium on Personal, Indoor and Mobile Radio Communications, 2004. (PIMRC 2004). (Vol. 3, pp. 1574 - 1578). Institute of Electrical and Electronics Engineers (IEEE).

[Link to publication record in Explore Bristol Research](#)
PDF-document

University of Bristol - Explore Bristol Research

General rights

This document is made available in accordance with publisher policies. Please cite only the published version using the reference above. Full terms of use are available:
<http://www.bristol.ac.uk/pure/about/ebr-terms.html>

Take down policy

Explore Bristol Research is a digital archive and the intention is that deposited content should not be removed. However, if you believe that this version of the work breaches copyright law please contact open-access@bristol.ac.uk and include the following information in your message:

- Your contact details
- Bibliographic details for the item, including a URL
- An outline of the nature of the complaint

On receipt of your message the Open Access Team will immediately investigate your claim, make an initial judgement of the validity of the claim and, where appropriate, withdraw the item in question from public view.

COMPARISON OF MIMO CHANNELS FROM MULTIPATH PARAMETER EXTRACTION AND DIRECT CHANNEL MEASUREMENTS

Arindam Pal, Chor Min Tan, Mark A. Beach

Centre for Communications Research, University of Bristol, UK. Email: A.Pal@bristol.ac.uk

Abstract - This paper presents a MIMO throughput performance analysis of dynamic wideband double-directional channel measurements that were recently obtained by the University of Bristol. Identical 16-element Uniform Circular Arrays (UCAs) were employed at both ends of the link and the parameters of the multipath components (MPCs) were extracted. In this paper, the performance analyses of several 4×4 subarrays of the 16×16 measurement arrays are presented. The MIMO response of these channels was synthesised from the extracted MPCs. A comparison is then made between the capacity estimates from the directly measured and synthesised MIMO channels. This was found to show good agreement.

Keywords – antenna arrays, multiple-input multiple-output, indoor propagation, channel models

I. INTRODUCTION

The theoretical performance benefits of deploying multiple antennas at both ends of a wireless communications link and the effect of channel correlation on MIMO capacity are well known [1-2]. However, accurate modelling of the wireless channel is needed for the development of practical MIMO applications, such as that needed for Wireless LANs. The so called “double-directional” approach of modelling the MIMO wireless channel is a well accepted method of providing a full description of the channel [3]. It can describe fading in the spectral, doppler, and spatial domains of the multi-dimensional signal vectors. This is achieved by making use of the joint distributions of radiated power in time, delay, directions of arrival (DOA) and direction of departure (DOD). The development of such models requires channel data in the form of multipath parameters from numerous propagation environments. This is ideally obtained from the extraction of multipath components (i.e. DOA, DOD, delay, power of each ray) from multi-element channel measurements.

In this paper, we present a capacity-based analysis of MIMO channels obtained from dynamic wideband channel measurements and double-directional multipath parameter extraction. The measurements were conducted with identical 16-element UCAs in indoor environments at 5.2 GHz. To the best of our knowledge, measurements of this scale have not yet been conducted elsewhere. This is probably due to

the hardware complexity of the measurement campaigns, and also the large computation time required for parameter extraction. Fortunately through UK Government funding under JERI 98 for measurement equipment facilities, and Toshiba TREL providing a state-of-the-art computer cluster, these difficulties have been overcome to a large extent at Bristol. The extracted multipath data allows us to investigate the interaction of different array geometries and element patterns within the measured environments. This type of knowledge is much needed to aid the design of antennas and antenna array topologies for future terminals employing MIMO capacity enhancement techniques. As an alternative to direct measurements, double-directional channel data can also be obtained from site specific models such as ray-tracing [4], or synthesised from power delay profiles (PDPs), Doppler power spectra (DPS) and power distributions in DODs and DOAs [5].

This paper is structured as follows. Section II gives a brief overview of the measurement campaign and the associated multipath parameter extraction. Section III contains a capacity based analysis of several 4×4 subarrays of the 16×16 measured channels, highlighting the importance of power normalisation. Section IV describes how MIMO wideband channel responses were calculated from the extracted MPCs using a plane-wave model, and a comparison between these values and the directly measured MIMO channels is also presented. Section V concludes the document.

II. CHANNEL MEASUREMENTS

A. Measurement Equipment

This measurement campaign was conducted alongside the Mobile VCE [6] campaign at the University of Bristol. The channel measurements were conducted using a Medav RUSK BRI channel sounder [7] capable of supporting multi-element wideband channel characterisation. The transmitter employs a periodic multi-tone signal with a bandwidth of 120 MHz, centred on 5.2 GHz and a repetition tone period of 0.8 μ s. The signal is constructed such that all tones have equal power and are evenly spaced over the measurement bandwidth. The patch antennas for the two identical 16-element UCAs were dual-polarised (horizontal and vertical), and were designed by the EM Group at Bristol [8]. Although these elements were dual-polarised facets,

only the vertical polarisation was considered during these measurements. Figure 1 shows the azimuth gain pattern of one of the antenna elements. The UCAs had a radius of 1.28λ .

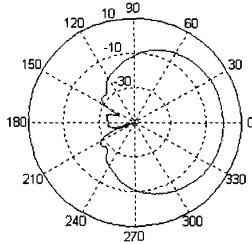


Figure 1: Azimuth gain pattern (dB) of an antenna

B. Measurement Environments

Dynamic measurements were conducted by slowly pushing the receiving UCA on a trolley, while the transmitting UCA was fixed at a certain location. Measurements were taken under different propagation conditions. This includes line-of-sight (LOS), obstructed LOS, non-line-of-sight (NLOS), populated scenario, unpopulated scenario, and different antenna heights at either end. Measurements were conducted in several indoor environments, including the foyer, corridor, research lab, open plan office and outdoor court yard. A full account of the measurement campaign and description of the environments can be found in [9].

C. Parameter Extraction

The newly developed hybrid-space Space Alternating Generalised Expectation-maximisation (HS-SAGE) algorithm [10] was used to extract multipath parameters of the channel, i.e. Direction of Arrival, Direction of Departure, time delay of arrival and complex amplitude of each ray from the transmit array to the receive array. Much of the development of the algorithm was conducted under the UK Mobile VCE Core 2 programme. In addition to being suitable for use with a circular array, it also enhances the effective processing speed of the classical SAGE algorithm [11] without sacrificing accuracy and resolution.

III. MIMO ANALYSIS OF MEASURED CHANNELS

A. Selected Antenna configurations

The purpose behind conducting measurements with 16-element circular arrays was to accurately characterise the multipath properties for the entire azimuth domain at both transmitting and receiving ends of a wireless link. For the purpose of capacity analysis, only certain 4×4 subsets of the 16×16 measurements have been used. A description of the chosen 4×4 sectors is now given below.

1) Facing and Non-Facing MIMO sectors

Most measurements were conducted with the circular arrays placed in line of sight. However, due to the shape and construction of the arrays and the relatively narrow beamwidth of the patch antennas deployed, some of the transmit-receive antenna pairs experienced a dominant LOS component, while other Tx-Rx pairs were effectively NLOS links. These were shielded by the ground planes of the arrays. See pictures of UCAs in [9] for further details.

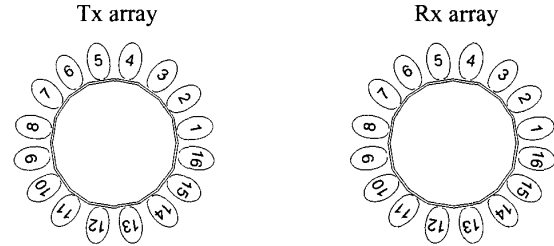


Figure 2: labelling of patch antennas in the 16-element measurement UCAs

From Figure 2, an example of a *facing* sector is (Tx 15,16,1,2 and Rx 7,8,9,10), whereas (Tx 7,8,9,10 and Rx 15,16,1,2) forms a *non-facing* MIMO sector. As expected, the *non-facing* channels were found to exhibit Rayleigh fading, aided by the large number of scatterers present in the indoor environment. The channels observed between *facing* arrays were found to follow a Ricean distribution with K-factors varying between 2-6 dB for the different environments considered. This justifies the use of *facing* and *non-facing* sectors to simulate LOS and NLOS MIMO scenarios respectively in the capacity analysis presented here.

2) Co- and Cross-oriented Antenna Arrays

It would be almost impossible to deploy an array comprising of omni-directional elements in any practical device, especially for a mobile terminal. It is likely that directional antennas such as the patch antennas (Figure 1) used in these measurements will be used in real MIMO application [12]. Due to their relatively narrow beamwidth, the effect of orientation of these elements must be taken into account.

The *facing* and *non-facing* sectors described in III.A.1) are *co-oriented* sectors. Since all 4 elements are facing a similar direction, the array is more likely to be entirely “shadowed” or “illuminated”. For contrast, we also observe the 4×4 MIMO channel for *cross-oriented* sectors, as given by elements 1,5,9,13 from each array in Figure 2. We define the “power spread” of a MIMO channel as the difference (dB) between the strongest and the weakest constituent SISO subchannels. This was found to be much greater for *cross-* than *co-oriented* sectors (Figure 6), indicating that *cross-oriented* channels were more likely to contain at least one strong constituent subchannel link.

The average *power spread* of the 4×4 *cross-oriented* channels was greater than 18 dB for all environments, including those where the UCAs were in NLOS (foyer loc 1, lab). As expected, *power spread* was even larger for smaller angular spreads, which was the case when a dominant LOS component existed (foyer loc 2, foyer loc 3, office). In either case, we observe that the orientation of the deployed antennas have a significant effect on the strength of the link in indoor propagation at 5.2 GHz.

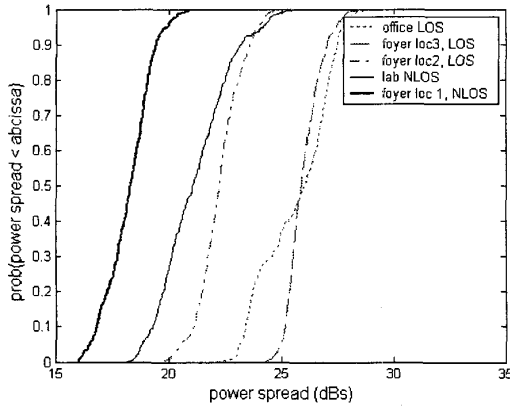


Figure 3: cumulative distribution functions (cdfs) of the power spread of cross-oriented subarrays

B. Channel Normalisation

The normalisation factor for each wideband measurement snapshot \mathbf{T}_i (i is the time or snapshot index) was calculated separately. This removed the effect of large-scale spatial fading, which can be significant for dynamic measurements, and ensured that only the small-scale spatial fading was observed. \mathbf{T}_i has dimensions of $N_R \times N_T \times N_F$, where N_R , N_T , and N_F are the number of receive antennas, transmit antennas and frequency components respectively.

Since adjacent elements in the UCAs are spaced at 0.5λ , constituent single-input single-output (SISO) channels could be assumed to experience sufficiently independent fading. Each 4×4 measured channel snapshot had dimensions of $(4 \times 4 \times 97 = 1552)$, thus providing a sufficient number of independent samples for normalisation. The normalised wideband channel \mathbf{H}_i was calculated from (1) and (2), where $\hat{\eta}_k$ is the normalisation factor estimate.

$$\hat{\eta}_k^2 = \frac{1}{n_R n_T N_F} \sum_{f=1}^{N_F} \sum_{j=1}^{N_R} \sum_{k=1}^{N_T} |\mathbf{T}_{i,f,j,k}|^2 \quad (1)$$

$$\mathbf{H}_i = \frac{\mathbf{T}_i}{\hat{\eta}_i} \quad (2)$$

The goal of channel normalisation is usually to scale the channel response so that the expectation of its power is

unity. This can be achieved by taking the summation in Equation (1) over only the 4×4 channel response that is being analysed. We refer to this as *unity-gain* normalization.

However, when comparing of performance of arbitrarily oriented directional antenna arrays at given locations of the transmitting and receiving arrays, we should ideally normalise for only the “omni-directional pathloss” between the two locations. This is equivalent to the pathloss measured when single omni-directional antennas are placed at the same transmit and receive locations. The *unity-gain* normalisation does not necessarily achieve this, especially for *co-oriented* directional antennas. Therefore, we introduce a *pathloss* normalisation factor.

Since the measurement UCAs propagate and receive over the entire azimuth range, the *pathloss* normalisation factor could be estimated from the average over all 16×16 constituent channels in Equation (1). However, the resulting normalised 4×4 channel is unlikely to have average gain of unity. The difference between the two normalisation techniques is demonstrated in Figure 4. The *unity-gain* normalisation can be used to observe that the 4×4 *facing* (LOS) channel is more correlated than the 4×4 *non-facing* (NLOS) channel at the same locations of the UCAs. On the other hand, *pathloss* normalisation shows better performance for the LOS channel despite higher correlation, simply because antenna sectors in line-of-sight receive more power. Thus, the two normalisation techniques deliver very different results, and either might be preferred depending on the purpose of the analysis.

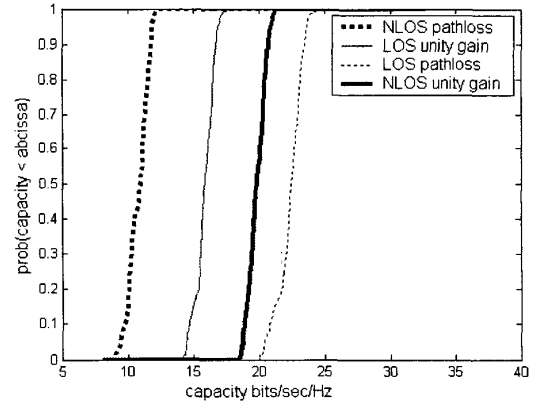


Figure 4: cdfs of normalised capacities calculated for *unity-gain* and *pathloss* normalisations, (SNR = 20dB), for 4×4 *facing* (LOS) and *non-facing* (NLOS) sectors

The omni-directional pathloss information may not always be available for measurements with directional antennas. In such cases, if transmit power across the transmit antennas is equal, the normalisation factor can be taken to be the gain of the strongest constituent SISO channel. This method gives

similar performance results as the *pathloss* normalisation for *cross-oriented* antennas.

C. Capacity Calculation

Since power was allocated equally to each transmit element and frequency sub-channel, and the frequency components were equally spaced, the capacity of the frequency selective channel was calculated using [1]

$$C_i = \frac{W}{N_f} \sum_f \log_2 \left(\det \left(\mathbf{I}_{N_R} + \frac{\rho}{N_T} \mathbf{H}_{i,f} \mathbf{H}_{i,f}^* \right) \right) \quad (3)$$

where $\mathbf{H}_{i,f}$ is the normalized channel response at frequency component f , $*$ is the complex conjugate, and ρ is the average signal-to-noise ratio (SNR) at each receiver branch over the entire bandwidth W . The normalised capacity of the wideband channel, given by C/W , will be presented in the remaining analysis.

IV. MIMO CHANNELS FROM EXTRACTED MULTIPATH PARAMETERS

A. Calculating MIMO response from extracted MPCs

Each snapshot of extracted MPCs describes the channel from the transmit origin to the receive origin as a joint function of the delays, DOAs and DODs. A summation of these electromagnetic wave components gives rise to the channel response. Applying the plane-wave propagation assumption allows us to predict the channel response for transmit and receive antennas placed at arbitrary locations that are close to their respective origins. In order to allow the plane-wave assumption to apply, the antenna arrays during measurements were placed at a sufficient distance from the nearest scatterers. Any effects of mutual coupling have been ignored. Equation (4) gives the channel response at each delay tap l ($l = 1..N_l$). N_l was chosen to be equal to the number of frequency tones employed in the measurements. The subscript l has been omitted in the rest of the equation (from $P_{s,l}$ and $\theta_{s,l}$) for clarity. For each snapshot, the multipath components were assigned to the nearest delay tap, according to their excess delay. The impulse response from the k th transmit to the j th receive element is given by

$$h_{j,k,l} = \sum_{s=1}^{N_s} \sqrt{P_s} e^{j\phi_s} \sqrt{G^{Rx}(\tilde{\theta}_s^A, \tilde{\varphi}_j)} \sqrt{G^{Tx}(\tilde{\theta}_s^D, \tilde{\varphi}_k)} \times e^{j2\pi(\tilde{x}_j^R \bullet \tilde{\theta}_s^A)} e^{j2\pi(\tilde{x}_k^T \bullet \tilde{\theta}_s^D)} \quad (4)$$

where N_s is the number of MPCs within each delay bin, P_s is the power of each path, and ϕ_s is the overall phase. Vectors \tilde{x}_j^R and \tilde{x}_k^T are the locations of the antenna elements defined with respect to the centres of the respective UCAs. $\tilde{\varphi}_j$ and $\tilde{\varphi}_k$ give the directions of orientation of antennas at

the Rx and Tx respectively. The locations and orientations were assigned to correspond to the 4×4 arrays described in III.A. Vectors $\tilde{\theta}_s^A$ and $\tilde{\theta}_s^D$ represent the DOAs and DODs respectively. Since DOAs and DODs were extracted as angles in the azimuth plane, elevation angles had to be assigned from a truncated statistical distribution. This was needed because angular spread in elevation can be expected to be significant due to reflections from the ceiling and the ground. $G^{Rx}(\tilde{\theta}_s^A, \tilde{\varphi}_j)$ and $G^{Tx}(\tilde{\theta}_s^D, \tilde{\varphi}_k)$ are the antenna pattern gains, which account for the arbitrary patterns and orientations of the antennas. The wideband channel response was calculated from windowed discrete-Fourier transform (DFT) of the tap-delay response $h_{j,k,l}$, and *unity-gain* normalisation was used for calculation of capacity.

B. Measured channels vs. extracted MPCs

Figure 5 shows a capacity comparison between MIMO channels from extracted MPCs and directly measurements for the 4×4 *facing* (LOS) and *non-facing* (NLOS) *co-oriented* sectors. The capacities of channels calculated from extracted MPCs were found to be lower than the measured channels for both LOS and NLOS scenarios. This has been found to be the case in similar studies conducted elsewhere [13]. This can be partly attributed to the limitations of the parameter extraction process. For instance, the total power of extracted parameters for any snapshot was typically about 70% of the measured power, as only a finite number (~ 50) of multipath components were extracted for each snapshot. Significantly larger computation time would have been necessary to extract a greater number of components.

The unextracted energy might be expected to consist mainly of a large number of low-power diffuse components and second/third bounce reflections. When the unextracted power was compensated for by adding low-power randomly distributed components (as suggested in [13]), there was much better agreement between the extracted MPCs and the measured channels (Figure 5). It can also be seen that the difference between the measured and estimated capacities is similar for the two antenna configurations, especially after addition of the “unextracted” components. The use of extracted parameters along with the plane wave model may not precisely predict the actual theoretical capacity. However, this approach may be potentially useful for comparing performances of different antenna types and array configurations. This has relevance to evaluation of candidate MIMO array designs [12], since extensive MIMO measurements are not easily realisable.

Figure 6 confirms that whilst the extraction process might fail to extract the low-power diffuse components, it accurately extracts the stronger MPCs, which make a greater contribution to the fading and the power of constituent SISO links. There is excellent agreement between the *power spread* of the MPC-based and measured channels, for both *co-* and *cross-oriented* antenna arrays.

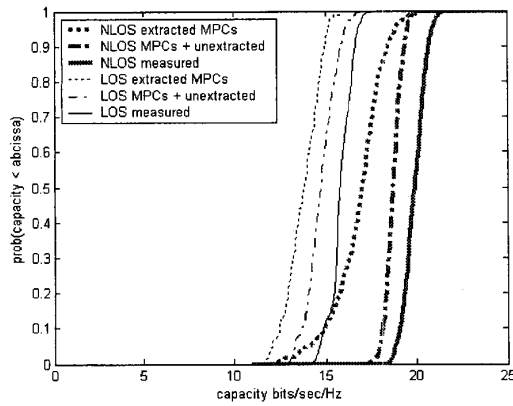


Figure 5: cdfs of normalised capacities (SNR = 20 dB) for 4x4 co-oriented antenna arrays. Propagation environment is the Foyer (location 2). Capacities from extracted MPCs, MPCs with added diffuse/noise components, and direct measurements are shown.

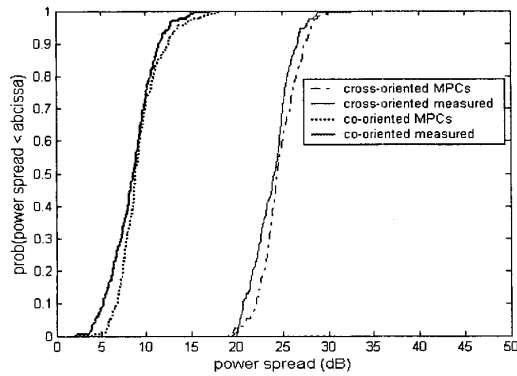


Figure 6: Power spread for 4x4 co- and cross-oriented arrays from measurements in Foyer (location 2) and extracted MPCs.

V. CONCLUSIONS

A performance based analysis of double-directional MIMO measurements has been presented. A comparison between measured channels and MIMO channels calculated from extracted multipath components was found to show good agreement, validating the experimental and parameter extraction process. The application of the extracted parameters from the HS-SAGE algorithm to the plane-wave model is potentially a useful tool for comparing the performance of array configurations in known propagation environments. This has much relevance to design of MIMO based devices.

ACKNOWLEDGMENT

Arindam Pal wishes to thank the UK ORS scheme and University of Bristol for his postgraduate scholarship.

REFERENCES

- [1] G. J. Foschini and M. J. Gans, "On Limits of Wireless Communications in a Fading Environment when Using Multiple Antennas", *Wireless Personal Communications*, pages 311-355, 1998.
- [2] D-S. Shiu, G. J. Foschini, M. J. Gans, and J.M. Kahn, "Fading Correlation and its effect on the Capacity of Multi-Element Antenna Systems", *IEEE International conference on Universal personal communications (ICUPC'98)*, vol. 1, pp. 429-433, October 1998.
- [3] M. Steinbauer, A. F. Molisch, and E. Bonek, "The Double-Directional Radio Channel", *IEEE Antennas and Propagation Magazine*, vol. 43, no. 4, pp. 51-63, August 2001.
- [4] B. S. Lee, A. R. Nix and J. McGeehan, "Indoor Space-Time Propagation Modelling Using a Ray Launching Technique", *IEE 11th ICAP*, Manchester, vol. 1, pp. 279-283, Apr. 2001.
- [5] L. Schumacher, K. I. Pedersen, and P.E. Mogensen, "From antenna spacings to theoretical capacities - guidelines for simulating MIMO systems," in *Proc. PIMRC Conf.*, vol. 2, pp. 587-592, Sept. 2002.
- [6] <http://www.mobilevce.com>
- [7] <http://www.channelsounder.de>, dated 10 January 2004.
- [8] D. L. Paul, I. J. Craddock, C. J. Railton, P. N. Fletcher, and M. Dean, "FDTD analysis and design of probe-fed dual-polarised circular stacked patch antenna", *Microwave and Optical Tech. Letters*, vol. 29, no. 4, pp. 223-226, May 2001.
- [9] M. A. Beach, C. M. Tan, and A. R. Nix, "Indoor Dynamic Double Directional Measurements", *International Conference on Electromagnetics in Advanced Applications*, Turin, Italy, 11 September 2003.
- [10] C. M. Tan, M. A. Beach, and A. R. Nix, "Multi-dimensional hybrid-space SAGE algorithm: Joint element-space and beamspace processing", *IST Mobile and Wireless Communications Summit 2003*, Aveiro, Portugal, 15-18 June 2003.
- [11] B. H. Fleury, M. Tschudin, R. Heddergott, D. Dalhaus and K. I. Pedersen, "Channel parameter estimation in mobile radio environments using the SAGE algorithm", *IEEE JSAC*, vol. 17, pp. 434-449, March 1999.
- [12] M. A. Beach, M. Hunukumbure, C. Williams, G.S. Hilton, P. Urwin-Wright, M. Capstick and B. Kemp, "An experimental evaluation of three candidate MIMO array designs for PDA devices", *COST 273/284 Workshop*, June 2004.
- [13] A. F. Molisch, M. Steinbauer, M. Toeltsch, E. Bonek, and R. S. Thoma, "Capacity of MIMO systems based on measured wireless channels", *IEEE Journal on Selected Areas in Communications*, vol. 20, pp. 561-569, April 2002.